Quantitative sampling using an Aerodyne aerosol mass spectrometer
1. Techniques of data interpretation and error analysis

James D. Allan,[1] Jose L. Jimenez,[2,3] Paul I. Williams,[1] M. Rami Alfarra,[4]
Keith N. Bower,[1] John T. Jayne,[5] Hugh Coe,[1] and Douglas R. Worsnop[5]

[1] The aerosol mass spectrometer (AMS), manufactured by Aerodyne Research, Inc., has been shown to be capable of delivering quantitative information on the chemical composition and size of volatile and semivolatile fine airborne particulate matter with high time resolution. Analytical and software tools for interpreting the data from this instrument and generating meaningful, quantitative results have been developed and are presented here with a brief description of the instrument. These include the conversion of detected ion rates from the quadrupole mass spectrometer during the mass spectrum (MS) mode of operation to atmospheric mass concentrations of chemical species (in $\mu g\ m^{-3}$) by applying calibration data. It is also necessary to correct for variations in the electron multiplier performance, and a method involving the measurement of the instrument's response to gas phase signals is also presented. The techniques for applying particle velocity calibration data and transforming signals from time of flight (TOF) mode to chemical mass distributions in terms of aerodynamic diameter ($dM/d\log(D_a)$ distributions) are also presented. It is also possible to quantify the uncertainties in both MS and TOF data by evaluating the ion counting statistics and variability of the background signal, respectively. This paper is accompanied by part 2 of this series, in which these methods are used to process and analyze AMS results on ambient aerosol from two U.K. cities at different times of the year. *INDEX TERMS:* 0305 Atmospheric Composition and Structure: Aerosols and particles (0345, 4801); 0394 Atmospheric Composition and Structure: Instruments and techniques; 0399 Atmospheric Composition and Structure: General or miscellaneous; *KEYWORDS:* aerosols, chemical composition, mass spectrometry, analysis techniques

1. Introduction

[2] Atmospheric particulate matter is known to have a major impact on phenomena such as climate forcing, heterogeneous chemistry, cloud formation, and the hydrological cycle [*Charlson et al.*, 1992; *Hitzenberger et al.*, 1999; *Jacob*, 2000; *Ramanathan et al.*, 2001; *Ravishankara*, 1997]. Urban areas in particular are known to be major sources of anthropogenic aerosol [*Colvile et al.*, 2001; *Mayer*, 1999], and the detrimental effects ambient particulate matter (PM) in cities has on visibility [*White and Roberts*, 1977] and the health of their inhabitants [*Dockery et al.*, 1993; *Künzli et al.*, 2000; *Nevalainen and Pekkanen*, 1998; *Schwartz*, 1994] have long been studied. The majority of environmental monitoring and control has been based around measuring the total mass of particulate matter based on the PM_{10} standard (particles of an aerodynamic diameter less than 10 μm) [*Department for Environment Food and Rural Affairs*, 2001; *Larssen et al.*, 1999], as these particles are more likely to pass the throat when inhaled. However, it has been suggested that the smaller particles, known as fine particles (the widely accepted definition being those of sizes less than 2.5 μm), are the more damaging to health, as they tend to have a higher toxicity and can penetrate deeper into the alveolar region of the lungs [*Harrison and Yin*, 2000; *Seaton et al.*, 1995]. This has led to the increased interest in fine PM and the adoption of the $PM_{2.5}$ standard in some areas such as the USA [*Environmental Protection Agency*, 1997].

[3] Our level of understanding of the nature, sources, processes and effects of atmospheric aerosols has so far been limited by the instrumentation that is available to study them. For a detailed review of such instrumentation, the reader is directed to *McMurry* [2000]. The technology to

[1]Department of Physics, University of Manchester Institute of Science and Technology, Manchester, UK.
[2]Department of Environmental Science and Engineering, California Institute of Technology, Pasadena, California, USA.
[3]Now at Department of Chemistry and Cooperative Institute for Research in the Environmental Sciences, University of Colorado, Boulder, Colorado, USA.
[4]Department of Chemical Engineering, University of Manchester Institute of Science and Technology, Manchester, UK.
[5]Aerodyne Research, Inc., Billerica, Massachusetts, USA.

accurately count, size, and determine the mass concentration of particles in real time is well established, but the chemical analysis of aerosol is not as easily performed. The most direct method is to collect particulate matter on a filter or impactor substrate over a period of hours and to analyze the material using standard analytical procedures, but this carries many intrinsic limitations. First, a measurable amount of material has to be collected, and the detection limits of laboratory chemical analysis instrumentation usually require sampling times from several hours to days, so temporal resolution is generally poor. Secondly, because of the time between sample collection and analysis, volatile components of the aerosol may evaporate and be lost or chemically unstable compounds may react. Semivolatile chemicals may also interchange with the gas phase during sampling. Thirdly, many impactor technologies separate particles aerodynamically to give some size-resolved information but the size resolution is limited to the number of stages in the impactor, and particle bounce may result in erroneous size information. Finally, because the aerosol is handled in bulk, no information on the extent of internal or external chemical mixing is retained.

[4] In recent years, the field of aerosol mass spectrometry has emerged to provide a real time method of the chemical analysis of aerosol. The principle is to introduce airborne particles into the instrument, vaporize the material, ionize the vapor molecules and then analyze the ions using mass spectrometry, according to their mass to charge ratio (m/z). *Suess and Prather* [1999] give a comprehensive history and review of the majority of instruments to date that use these principles. Several approaches have been used, but much work over the last decade has focused on the combination of laser desorption and ionization (LDI), first introduced by *Sinha* [1984], with a time of flight mass spectrometer [e.g., *Murphy and Thomson*, 1995; *Prather et al.*, 1994]. The basic principle is to use a high-powered pulsed laser to both vaporize and ionize individual particles and obtain a mass spectrum of their components. Most implementations involve accelerating the aerosol through a nozzle and forming a collimated particle beam. The measured velocity of the particles can be used to determine the aerodynamic size. This allows, for the first time, detailed information on particle size and chemical information to be obtained in real time [e.g., *Liu et al.*, 1997; *Murphy et al.*, 1998; *Silva and Prather*, 1997].

[5] While much qualitative data on the chemical composition of aerosol can be attained, providing quantitative information with LDI is difficult, as particles are not necessarily completely desorbed and are detected with greatly varying efficiency depending on their size and chemical nature [*Allen et al.*, 2000; *Kane and Johnston*, 2000]. As the particles are detected and counted optically, particles of around 200 nm and smaller are not counted reliably. Also, information on more complex organic chemicals is lost due to the extensive molecular fragmentation caused during the combined desorption and ionization and the low ionization efficiency of LDI on aliphatic chemicals and their derivatives [*Silva and Prather*, 2000], although the two-stage technique introduced by *Morrical et al.* [1998] does mitigate the fragmentation issue by using two weaker laser pulses to perform the desorption and ionization separately.

[6] The aerosol mass spectrometer introduced by *Jayne et al.* [2000] (hereafter referred to as the AMS) and developed by Aerodyne Research, Inc. (ARI), attempts to address the issue of quantifying the mass concentrations of chemical species present in aerosol. It builds on principles used in the instrument described by *Allen and Gould* [1981] and is similar in nature to that described by *Tobias and Ziemann* [1999], in that it vaporizes particles on a heated surface and employs quadrupole mass spectrometry with electron impact ionization (EI). The ionization works by impacting gas phase molecules with 70 eV electrons emitted from a Tungsten filament. Although EI produces some fragmentation of the molecules, the technique is well established in analytical chemistry, so known chemicals create a highly reproducible response that can be related to the molecular structure [*McLafferty and Turecek*, 1993]. The instrument also uses an aerodynamic lens [*Liu et al.*, 1995a, 1995b] in its inlet system, so that particles are introduced into the instrument at near 100% efficiency over a range of sizes, depending on the specifications of the lens design used.

[7] A quadrupole mass spectrometer, while allowing quantitative data collection [*Bley*, 1988] and the high time resolution required for particle sizing, does carry the intrinsic limitation that ions of only one m/z can be studied at any one time. This means that complete mass spectra of individual particles cannot be obtained using this method, but instead quantitative information regarding the entire aerosol ensemble is acquired. Bearing this in mind, the results from this instrument are different in nature from those produced by time of flight mass spectrometry instruments and should therefore be viewed as complementary.

[8] In this paper, we present a suite of analysis tools that have been developed for producing quantitative results, and in the companion paper [*Allan et al.*, 2003], results from experiments in two U.K. cities (Edinburgh during November 2000 and Manchester during June 2001 and January 2002) are presented, interpreted, and compared.

2. Instrument Description

[9] A fuller description of the AMS and its operation is given by *Jayne et al.* [2000] and *Jimenez et al.* [2003], but a brief description of the instrument owned by the University of Manchester Institute of Science and Technology (UMIST) is given here.

[10] Figure 1 shows the basic layout of the instrument. A critical orifice controls the flow into the instrument, and diameters of 100 and 120 μm have been used, which give nominal inlet flow rates of about 1.5 and 2.0 cm^3 s^{-1}, respectively. The flow rate is monitored by a laminar pressure drop element. The aerodynamic lens design is identical to that used and described by *Jayne et al.* [2000], which focuses particles into a tightly collimated beam by passing through a series of apertures, before accelerating them through a nozzle. In its original configuration the particles between the approximate aerodynamic diameters of 70 and 600 nm are focused with near 100% efficiency, allowing quantitative study of the majority of accumulation mode aerosol particles. A later modification to the lens design reduced the lower cut-off to approximately 30 nm. Particles smaller than the lower limit are too small to be aerodynamically focused, and the majority are

Particle Beam   Aerodynamic Sizing   Particle
Generation   Composition
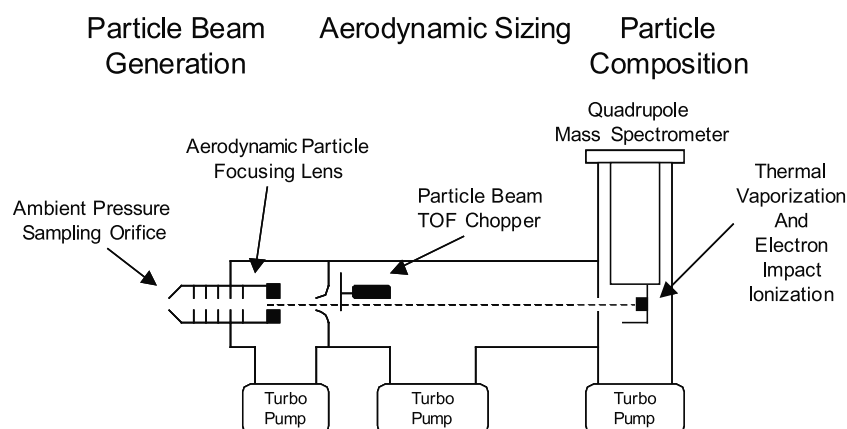
Figure 1. Basic schematic of the Aerodyne aerosol mass spectrometer.

not collimated into the beam. Particles larger than the upper limit tend to impact on the lens stages, which results in the transmission efficiency decreasing with increasing diameter beyond that size. Laboratory work has shown that several cases of nonspherical (e.g., ammonium nitrate) as well as spherical particles are well focused by the lens [*Jayne et al.*, 2000]. However, it is recognized that highly nonspherical particles such as chain agglomerates may not be focused efficiently [*Liu et al.*, 1995b]. These effects are the subject of ongoing work that will be presented in a future publication.

[11] A skimmer cone removes most of the gas from the sample flow before the aerosol beam enters the second differentially pumped chamber. However, it must be noted that the majority of the mass contained within the beam (by a factor of about $10^2 – 10^3$) is still gas phase rather than particle phase. The beam then passes a chopper wheel, which consists of a rotating disc with two radial slits positioned on a mount that is actuated by a servo. The chopper can either let the beam pass freely (the "open" position), completely block it (the "blocked" position, used for background measurements) or let small packets of material through at a user-definable rate of $100 – 150$ cycles per second (known as the "chopped" position). The position used depends on the mode of operation of the instrument. The second chamber acts as a time of flight region for particles so their velocity can be calculated from the time taken to reach the detection region after passing the chopper.

[12] The third chamber follows the TOF region and contains a subchamber that houses the detection region. Each chamber has its own turbomolecular pump, and the differentially pumping the chambers reduces the sampled gas flow from the lens such that the particle mass is concentrated by a factor of 10^7 compared to the ambient air. In this way, with the exception of the major components of air (e.g., N_2, O_2, Ar, H_2O, and CO_2), there is no detectable interference of vapor components in the measured particulate mass spectrum. Particles are impacted on a heated surface (either a flat molybdenum surface coated with layers of molybdenum mesh or an inverted cone made from porous tungsten have been used), where they flash vaporize. Temperatures used range from 400°C to 950°C but are generally kept constant during a measurement campaign. The resulting vapor plume is ionized by EI,

and then positive ions are introduced into a quadrupole mass spectrometer. Balzers models QMA 400 and QMA 410 have been used on different occasions. This selects ions according their *m/z* before their detection by an electron multiplier. The signal from the multiplier is fed through a preamplifier to a National Instruments data acquisition system in the logging computer. The voltage is sampled at rates of up to 5 MHz by the data acquisition system and is processed and recorded at a user definable rate by the logging software (up to 100 kHz, but 20 kHz was used for the work described here).

[13] Because the laser pulses used in LDI act to perform both desorption and ionization simultaneously, they must be of a high power, which results in extensive fragmentation of the molecules. Thermal flash vaporization is gentler, so little chemical fragmentation occurs before the constituents are ionized. This also means that low volatility solid particulate matter is not desorbed and therefore not detected, and hence the instrument in the configuration described here cannot measure aerosol components such as sea salt, crustal material, or elemental carbon. Volatile and semivolatile solid or liquid particles such as those composed of ammonium nitrate or sulfate or organic carbon are detected efficiently.

[14] The instrument alternates between two modes during operation, mass spectrum (MS) and time of flight (TOF) mode, by default spending 20 s on the former and 40 s on the latter during a cycle. The data are typically averaged over periods of between 5 and 30 min.

[15] During MS mode operation in the default configuration, the chopper alternates between the open and blocked positions every 5 s, while the mass spectrometer continuously scans between 0 and 300 Daltons at a rate of 1000 Daltons per second. A mass spectrum of the particle and gas beam is obtained by subtracting the average mass spectrum acquired when the chopper is in the blocked position from the average when the chopper is in the open position. This removes any contribution from background gas in the detector (the operating pressure in the detection region is $<10^{-7}$ torr). Ambient mass concentrations (in $\mu g\ m^{-3}$) for chemical species can be derived from the mass spectra.

[16] During TOF mode operation, the mass spectrometer is set to a single *m/z* and sampled at a user-definable rate (20 kHz in this case). The spinning chopper is moved into the chopped position and an optical sensor positioned on the chopper mount senses when a slit is in the position

where aerosol beam is allowed to pass. This provides 400 separate measurements of the detector response over a single chopper cycle. The delay time between the particle-laden slug passing through the chopper and the ion detection in the mass spectrometer is the particle time of flight through the system. By summation of signals in each measurement channel over many chopper cycles a signal distribution of the *m/z* can be obtained. As the time of flight is dependent on the particle's aerodynamic diameter, these data are then used to calculate mass distributions for a particular chemical as a function of aerodynamic diameter.

[17] A data analysis suite to apply the quantification procedures on the raw AMS data and yield calibrated size and mass aerosol data has been developed using the Igor Pro data analysis software (Version 4.05A, WaveMetrics, Inc., P.O. Box 2088, Lake Oswego, Oregon 97035, USA) with the intention of being versatile enough to be applied to all data sets acquired by the instrument.

3. Data Interpretation: Quantification of Mass

[18] An important feature of the AMS is the ability to equate a response (detected ion rate) in the mass spectrometer to a mass concentration of a given species in a sample. The data acquired by the logging computer are the voltage outputs from the preamplifier, which are proportional to the electrical current outputs of the electron multiplier detector. The latter are converted to detected ion rates by dividing by the average single ion signal strength. This quantity is dependent on the gains of both the preamplifier and the multiplier and is measured as part of the calibration protocol. The aerosol beam is blocked and the ionizer filament current reduced, so that individual ions, created from the background gas phase material, can be distinguished as electrical pulses and measured. This calibration is performed daily during continuous operation.

[19] The continuous mass spectrum must also be converted into discrete *m/z* channels in order to be interpreted. The quadrupole is configured so that during scanning, *m/z* signals form distinct peaks in a mass spectrum with well-defined flat tops. The plateaus have widths of approximately 0.45 Daltons, and the averaged height is taken to be the detected ion rate for that *m/z*.

[20] To convert an ion rate signal *I*, to an ambient mass loading *C*, the following generalized formula is applied, following *Jimenez et al.* [2003], which is, in turn, adapted from *Bley* [1988].

$$C = \frac{1}{IE}\frac{1}{Q}\frac{MW}{N_A}\cdot I,$$ (1)

where MW is the molecular weight of the parent species, N_A is Avogadro's number, Q is the volumetric flow rate into the instrument, and IE is the ionization efficiency, a dimensionless quantity equaling the ratio of ions detected by the multiplier to the number of available desorbed molecules of the parent chemical species. Note that the IE depends both on the ionization efficiency for producing charged ions and the transmission efficiency of the ions passing through the quadrupole mass spectrometer.

[21] Molecules of most chemical species undergo fragmentation during ionization. For example, there are two

major nitrate peaks in the mass spectrum of ammonium nitrate aerosol at *m/z* = 30 (NO^+) and *m/z* = 46 (NO_2^+). To measure the total mass of nitrate, both fragments must be summed as follows:

$$C_{NO_3} = \frac{1}{IE_{NO_3}}\frac{1}{Q}\frac{MW_{NO_3}}{N_A}\cdot\sum_{f=30,46}I_f$$ (2)

[22] The ionization efficiency of nitrate, IE_{NO3}, is determined during routine calibration, as described by *Jayne et al.* [2000]. Ammonium nitrate particles are generated from an aqueous solution using a nebulizer or collision atomizer and size selected using a Vienna design differential mobility analyzer (DMA) [*Winklmayr et al.*, 1991]. By applying the density of ammonium nitrate (1.725 g cm^{-3}) and a measured shape factor of 0.8 to the spherical volume associated with the diameter selected (normally 300–350 nm, so that individual particles can be reliably distinguished and counted), the average mass of the singly charged particles is calculated. This is then compared to the average integrated signal pulse produced by single particles in the instrument to calculate the ionization efficiency. Multiply charged particles are eliminated from this calibration analysis by running the instrument in TOF mode and ignoring particles with a time of flight greater than a threshold value, i.e., with too large an aerodynamic diameter. Additionally, the strength of the solution (normally 0.015–0.03 mol dm^{-3}) is chosen to result in more dry particles of the desired size being produced compared to the multiply charged sizes.

[23] The signal strengths of the MS and TOF modes are also compared and checked for consistency to ensure the instrument is configured and working correctly. However, the signal is expected to be slightly higher in MS mode for the generated particles as this includes the mass of the multiply charged particles. The number of particles counted by the AMS is also compared with a condensation particle counter (CPC) to verify efficient particle transmission.

[24] This calibration can also be applied to other chemical species by summing the *m/z* channels that correspond to the fragments arising from the ionization of that species. The assumption is that the ionization cross section of the parent molecules is proportional to the number of electrons present [*Jimenez et al.*, 2003; P. J. Silva, Aerodyne Research, Inc., unpublished laboratory data, 2001]. If it can be assumed that this, in turn, is proportional to the molecular weight, the following generalization can be made about a chemical *x* when compared to nitrate:

$$\frac{MW_x}{IE_x} = \frac{1}{k_c}\frac{MW_{NO_3}}{IE_{NO_3}},$$ (3)

where k_c is a dimensionless constant, specific to the chemical species type. This means that the mass calculation formula for nitrate can be applied to other chemical species by multiplying by k_c and using the values and , providing that all *m/z* components of the species have been identified. The k_c factor has been found experimentally to be equal to 1 for most inorganic chemicals, approximately 2 for simple

hydrocarbons, and 1.5 for more oxidized organic molecules (M. R. Alfarra, UMIST, unpublished laboratory data, 2002; P. J. Silva, Aerodyne Research, Inc., unpublished laboratory data, 2002).

[25] An additional correction factor will have to be applied if summing all the appropriate m/z channels is not possible, for instance, if one or more receives signals from other chemical species. This will still yield meaningful data, as the fragment pattern for a chemical under given heater and ionizer conditions is repeatable [*Jimenez et al.*, 2003] and can be determined in the laboratory.

[26] When summing m/z channels, the correction described by the equation 4 should be applied to take account of varying instrument response for different m/z values. This is independent of chemical species and is taken from *Jimenez et al.* [2003].

$$I_{m/z}^{\text{corrected}} = \frac{I_{m/z}^{\text{measured}}}{T_{m/z}G_{m/z}}, \tag{4}$$

where $I_{m/z}$ is the signal intensity as a function of m/z, $T_{m/z}$ is the relative transmission of the quadrupole and $G_{m/z}$ is the relative gain and detection efficiency of the electron multiplier. This correction has not been applied to the data presented here or in the accompanying paper [*Allan et al.*, 2003], as the relative transmission of the quadrupole as a function of m/z has not yet been measured, though should be a minor correction according to the manufacturer.

[27] Because a finite number of ions are being detected, there will be an intrinsic variability in the average number detected. As the number of available molecules is high but the probability of successfully ionizing and detecting a specific molecule is low, it can be assumed that the probable distribution of numbers detected for a given population can be modeled as a Poisson distribution. The standard deviation of this distribution is equal to the square root of the product of the number of available molecules and the probability of detection [*Stroud*, 1987]. This product should be approximately equal to the average number of ions detected during the sampling period. Using this approach, the error associated with a signal I, in counted ions per second, can be estimated as follows:

$$\Delta(It_s) = \alpha\sqrt{It_s} \therefore \Delta I = \alpha\frac{\sqrt{I}}{\sqrt{t_s}}, \tag{5}$$

where t_s is the amount of time, in seconds, spent sampling a particular m/z channel. Note the time will have to include the averaging period, the scanning rate (1000 Daltons s^{-1}) and the averaging window size (0.45 Daltons). Here α is a factor applied to account for the fact that the signal from a single ion is not a constant but arises from a Gaussian distribution of pulse areas. The relative standard deviation of this distribution has been determined in the laboratory to be about 0.68 for one type of multiplier detector (and can be readily determined for a different detector by the data acquisition software). By convolving this Gaussian with the Poisson distribution, α is given the value 1.2.

[28] Note that this error applies to a single "open" or "blocked" signal. In order to calculate the error on the "difference" signal, which is the arithmetic subtraction of the "blocked" from the "open," the errors must be summed in quadrature as follows:

$$\Delta I_d = \sqrt{\Delta I_o^2 + \Delta I_b^2} = \alpha\frac{\sqrt{I_o + I_b}}{\sqrt{t_s}} \tag{6}$$

[29] A further correction must be made when viewing data as a time series. Over time, the performance of the electron amplification chain in the multiplier slowly degrades, reducing the magnitude of the signal generated per ion detected. The relative degradation should be uniform for all parent chemicals, so a correction factor can be calculated by inspecting the signals due to the air beam that enters the instruments with the aerosol sample (either $m/z = 28$, which corresponds to N_2^+ or $m/z = 32$, which corresponds to O_2^+), which would be constant in ambient air if the amplification of the ion signal did not decrease with time. The flow rate should also be included in the calculation, as this may vary during a sampling period (due to the inlet critical orifice becoming partially blocked with debris or changing size due to temperature fluctuations) and alter the amount of air reaching the detection region. However, the flux of air entering the center of the skimmer and ultimately reaching the ionization region is dependent on the morphology of the gas expansion at the nozzle and is therefore not necessarily directly proportional to the flow rate. Instead, the following approximation is used:

$$AB \propto Q + Q^*, \tag{7}$$

where AB is the signal due to the air beam (in detected ions per second), Q is the volumetric inlet flow rate, and Q^* is a constant offset. This was evaluated in the laboratory by replacing the pinhole with a needle valve and adjusting the flow rate. It was found that the approximation applied for flow rates above 0.5 cm^3 s^{-1} with Q^* equal to 0.68 cm^3 s^{-1}. Below 0.5 cm^3 s^{-1}, AB is not linear with flow rate.

[30] Using these assumptions, a dimensionless correction factor is obtained as a function of time (t), which is applied to all signals recorded by the AMS and is calculated using the following equation:

$$I_t^{\text{corrected}} = I_t^{\text{measured}} \cdot \frac{AB_o(Q_t + Q^*)}{AB_t(Q_o + Q^*)}, \tag{8}$$

where AB_t and Q_t are the air beam strength and flow rate measured at time t and $t = 0$ is considered to be the time of (or shortly after) a calibration. The value of the correction factor can be seen as a ratio of the multiplier gain during calibration and the multiplier gain as a function of time. An example of this is shown in Figure 2. The points where the calibration factor returns to unity are the occasions when electron multiplier calibrations were performed. The points where the correction factor does not return to exactly 1 may be due to either the tolerance of the calibration or variations in the ion collection efficiency (i.e., the fraction of available ions successfully detected rather than the strengths of the signals generated) through
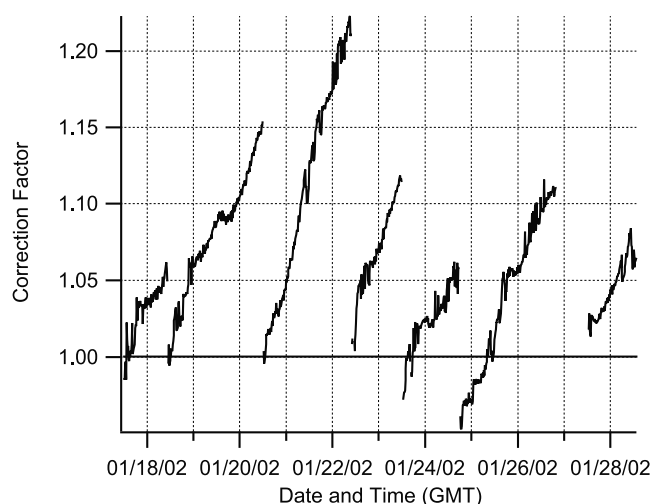
Figure 2. An example of the correction factor applied during a campaign to offset variations in multiplier performance, based on the strength due to the air signal. (Manchester, U.K., January 2002) The points where the factor returns to 1 are due to recalibrations.

the electron multiplier's working lifetime. Neither of these factors will affect the end results of the calculations, as the correction process will account for both phenomena.

4. Mass Spectrum Mode Results

[31] Figure 3 is an example of part of the mass spectrum (up to $m/z = 100$) of an aerosol ensemble, measured during November 2000 at Edinburgh, U.K. Note that the largest peaks are due to the gas phase component of the beam.

The peaks due to nitrate at $m/z = 30$ (NO^+) and 46 (NO_2^+) are shown, as are those due to sulfate at $m/z = 48$ (SO^+), 64 (SO_2^+), 80 (SO_3^+), 81 (HSO_3^+), and 98 ($H_2SO_4^+$). There are numerous peaks that are attributed to organic chemicals in the ensemble, so only the major ones are indicated ($m/z = 44$, 43, 55, 57, 69, 71, and 91). Of particular interest is $m/z = 91$, which is a common fragment of aromatic compounds. Also of note is $m/z = 44$, which corresponds to the CO_2^+ ion. While there is some contribution to this from gas phase carbon dioxide, the majority of the signal typically comes from particle phase organic chemicals so it is labeled as such. There are several organic peaks below $m/z = 43$ that bear significant amounts of mass but are not labeled for the purpose of clarity, such as $m/z = 26$, 27 and 29. The peaks $m/z = 15$, 16, 17, and 18 contain signals due to ammonium and water in the particle phase, but these are difficult to study, as they receive interference from each other and fragments of gas phase material, most notably the O^+ fragment ($m/z = 16$) from oxygen. The methods for deriving data from these peaks are currently under development and will be the subject of a later paper.

[32] The standard deviations associated with the m/z channels were calculated using the methods discussed above and are shown on the graph as the lower end points of the sticks.

[33] The corresponding loadings of nitrate, sulfate and organics calculated using the method discussed above for the data from Edinburgh during November 2000 are shown in Figure 4. For nitrate, the m/z channels 30 and 46 were summed. For sulfate, 48, 64, 80, 81, and 98 were identified as the m/z channels bearing the mass. While 48 and 64 have a high signal to noise and are known not to receive significant interferences from other ambient species, the signals at 80, 81, and 98 are smaller (see Figure 3) and contain an amount of signal from organic chemicals. The ratios of the signals at $m/z = 80$, 81, and 98 to

Figure 3. An example of part of an aerosol ensemble mass spectrum. (Edinburgh, U.K., November 2000) The full mass spectrum (up to $m/z = 300$) is not included for clarity. The lower ends of the sticks correspond to the calculated 1σ uncertainty in the signals. Peaks due to organic chemicals are denoted as "Org."
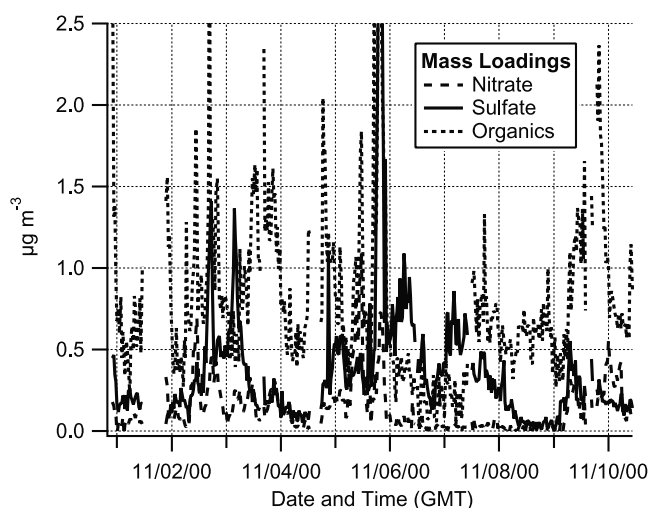
Figure 4. An example of calculated mass loadings for sulfate, nitrate, and total organics. (Edinburgh, U.K., November 2000) The large event on 5 November is due to a firework plume. This data set is discussed in more detail by *Allan et al.* [2003].

the summed signal at 48 and 64 were inspected and found to be largely invariant, except during periods of high organic activity relative to sulfate. To account for this interference, the sulfate contributions at m/z = 80, 81, and 98 were calculated based on the signals at m/z = 48 and 64 and the ratios obtained from periods of high sulfate but low organic activity (0.12, 0.1, and 0.057, respectively). A correction factor of 2.5 was applied to the sulfate loading as this has been found to provide results most closely matching other independent measurement techniques, such as those based on in situ and offline ion chromatography technologies [*Allan et al.*, 2003; *Jimenez et al.*, 2003; M. R. Canagaratna, Aerodyne Research, Inc., unpublished field data, 2000; F. Drewnick et al., Intercomparison and evaluation of four semi-continuous PM-2.5 sulfate instruments, submitted to *Atmospheric Environment*, 2002]. Part of this factor arises because a small amount of signal due to sulfate manifests at m/z = 32, which receives interference from oxygen (O_2^+) in the air and therefore cannot be summed. However, by analyzing ammonium sulfate aerosol carried in pure nitrogen, it was found that this fragment contributed only 7.2% of the total signal due to sulfate, so the contribution from this phenomenon will be small. It may also partly be due to a low relative ionization cross section (k_c) for ammonium sulfate, but preliminary experiments have shown this to be close to unity (F. Drewnick, University at Albany, State University of New York, personal communication, 2002).

[34] The factor does appear to be repeatable across field campaigns and AMS units and the comparisons with other instruments cited above have shown very good agreement. While it works well, the precise reason this factor needs to be included is at present unclear and is currently being investigated.

[35] The total organic mass loading is obtained by summing all the peaks in the mass spectrum except those known to originate from inorganic species and those below m/z = 12 (C^+). Peaks subtracted include those associated with nitrate, sulfate, air, water, ammonium, hydrogen chloride, sodium, and potassium. A correction factor of 0.7 is applied, based the study of various organic chemicals in the laboratory (M. R. Alfarra, UMIST, unpublished laboratory data, 2002; P. J. Silva, Aerodyne Research, Inc., unpublished laboratory data, 2002). This is the reciprocal of the k_c factor mentioned previously. It must be again stressed that this is a measure of semivolatile and volatile material only and that it is of the total mass of the organic species, not just carbon. Therefore the data obtained are conceptually similar but should not be expected to be equal to the masses of total organic carbon (TOC) measured with other techniques. This instrument is not expected to be able to observe pure elemental carbon (EC), due to its low volatility. The techniques for identifying and quantifying organic chemicals based on AMS data are currently still under development, but initial external comparisons have proved promising (M. R. Canagaratna, Aerodyne Research, Inc., unpublished field data, 2000).

5. Data Interpretation: Quantification of Size

[36] When the instrument is run in time of flight (TOF) mode and the detector response is displayed as a function of
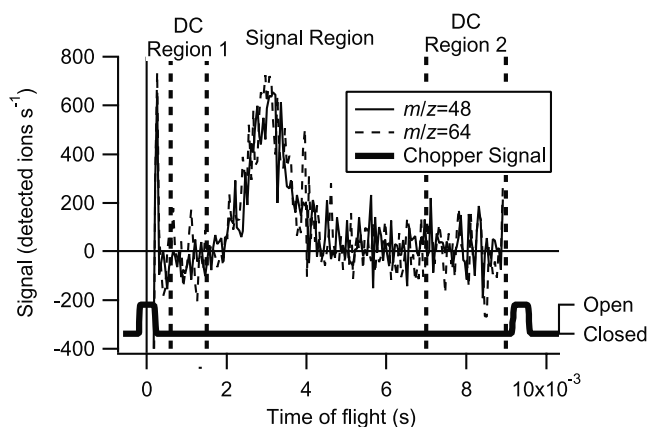
Figure 5. An example of the data produced in time of flight mode. (Edinburgh, U.K., November 2000) The signal from the chopper sensor is also shown on the same time axis. The two DC regions are where the baselines and the errors of the signals are calculated.

particle time of flight at a fixed m/z, a size distribution for a particular chemical species can be obtained such as that presented in Figure 5. The area under the graph represents the average number of ions detected per chopper cycle and can be converted to total mass, using the same mathematical method as before but including the chopper frequency and slit width information to compensate for the smaller fraction of the total particle beam sampled in TOF mode compared to MS mode.

[37] The zero in a TOF trace is evaluated in two regions, shown in Figure 5 as the ''DC regions,'' where no particles are expected to be detected. These correspond to particle velocities that are too low or too high to be transmitted into the instrument. This evaluation of the baseline removes the contribution to the signal from background gas phase material in the detection region. The need for a particle-free region at the end of the TOF period determines the maximum chopper frequency at which the instrument can be operated. There will be noise on the signal due to the background ion signal in any particular m/z channel, which is subject to the random nature of the ion detection as discussed earlier. The noise can be evaluated by calculating the standard deviation of the signal data points within the DC regions. Note that in some m/z channels such as 15, which have a contribution from both a gas phase signal ($^{15}N^+$ in this case) and a particle signal (e.g., NH^+ from ammonium), the front DC region is contaminated by the gas-signal and is excluded from the analysis.

[38] It is clearly of interest to know the mass distribution as a function of aerodynamic diameter. The aerodynamic diameter of a particle for a given sizing method is defined as the diameter of a sphere of unit density (1 g cm^{-3}) that would reach the same velocity as the subject particle during sizing. In this case, the particle acceleration mainly occurs at the nozzle. A velocity calibration is performed as described by *Jayne et al.* [2000] except the fit function has been modified to include the particle velocity prior to acceleration through the nozzle (J. L. Jimenez et al., Size resolution of the aerosol mass
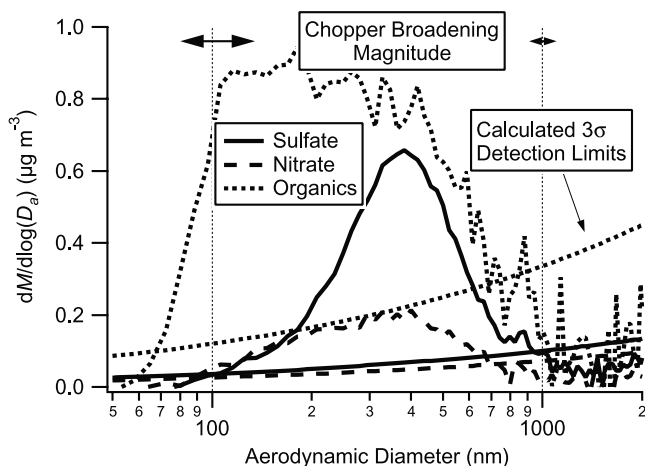
Figure 6. An example of calculated mass distributions of nitrate, sulfate, and organics. (Edinburgh, U.K., November 2000) The detection limits shown are calculated from the standard deviation of signals within the DC regions in Figure 5. The chopper broadening magnitudes are indicated by horizontal arrows at 100 and 1000 nm aerodynamic diameter relating to a 3.5% chopper operating at approximately 100 Hz, giving a time of flight uncertainty of ±0.175 ms.

spectrometer, manuscript in preparation, 2003) (hereinafter referred to as Jimenez et al., manuscript in preparation, 2003)

$$\nu_p = \frac{L_c}{t_p} = \frac{\nu_g - \nu_l}{1 + (D_a/D^*)^b} + \nu_l. \qquad (9)$$

where ν_p is the particle velocity, L_c is the particle flight length, t_p is the particle time of flight, D_a is the particle aerodynamic diameter, ν_g is the gas velocity on exiting the nozzle, ν_l is the gas velocity within the aerodynamic lens, and D^* and b are calibration constants.

[39] The ion rate as a function of time of flight, I_{tp}, can be transformed to $\log_{10}$ diameter space, $I_{\log(D_a)}$ using equation (10). This approach treats the detected ion rate as dN_I/dt_p, where N_I is the average total number of ions detected per TOF period (i.e., the area under the curve in Figure 5) and is maintained during the transformation.

$$\log(D_a) = \log(D^*) + \frac{1}{b} \log \left(\frac{\nu_g - \nu_l}{(L_c/t_p) - \nu_l} - 1 \right)$$

$$I_{\log(D_a)} = \frac{dN_I}{d\log(D_a)} = \frac{dN_I}{dt_p} \cdot \frac{dt_p}{d\log(D_a)} \qquad (10)$$

$$= I_{t_p} \cdot \left[2.3026 \cdot b \left(a_o + a_1 t_p + a_2 t_p^2 \right) \right]$$

$$a_0 = -\frac{L_c}{\nu_g - \nu_l} \quad a_1 = 1 + 2\frac{\nu_l}{\nu_g - \nu_l} \quad a_2 = -\left(1 + \frac{\nu_l}{\nu_g - \nu_l} \right) \frac{\nu_l}{L_c}$$

[40] The detected ion distribution in $\log_{10}$ diameter space can then be easily converted to a mass distribution ($dM/d\log(D_a)$) by normalizing to the total mass concentration calculated from the MS mode data; Figure 6 shows an example of this. The normalization serves to correct the integral of the trace if not all of the m/z channels corresponding to a chemical species are being scanned in TOF mode. An indication of the detection limit associated with the signals has also been included in Figure 6. This is 3 times the standard deviation of the data points within the DC regions as discussed above, transformed into $\log_{10}$ diameter space.

[41] This distribution should, if a particle density can be assumed or derived from the composition, be comparable with a volume ($dV/d\log(D_p)$ or $n_v(D_p)$) distribution that can be derived from other sizing instruments [*Seinfeld and Pandis*, 1998]. However, it is expected that the mode aerodynamic diameter measured by the AMS will not necessarily agree with the diameters obtained using different sizing techniques such as optical particle counters (OPCs) or differential mobility analyzer (DMA) based instruments (e.g., differential mobility particle sizer, scanning mobility particle sizer). Perfect size agreement with other instruments that employ aerodynamic methods such as aerodynamic particle sizers (APSs) or cascade impactors is also not expected. This is because the sizing is performed at a much lower pressure in the AMS, meaning that the measured particles are in the free molecular regime rather than in the transition regime. This leads to the aerodynamic diameters of particles measured by the AMS to be related to their physical diameters by the particle density, ρ, rather than by $\rho^{1/2}$, as observed by other instruments.

[42] There are uncertainties to the sizing, most notably due to the fact that larger particles take a finite time to vaporize, and that the chopper slit has a finite width. As a result of the latter, the time of flight has an uncertainty arising from defining the start time of the particle flight. Both effects combine to broaden the distribution. Uncertainties due to the time taken for gas phase molecules to be ionized after vaporization and for the ions to pass through the quadrupole are assumed to be negligible. These issues are discussed in more detail by Jimenez et al. (manuscript in preparation, 2003).

[43] Note that the mass distribution shown in Figure 6 is not corrected for the size-dependent lens transmission function described by *Jayne et al.* [2000] because this is not possible without first removing the broadening effects mentioned above. The methods for effectively performing this are currently under development.

[44] Using these techniques, quantitative information on how chemical components are distributed among particle sizes can be obtained with a resolution in both size and time that is not conventionally achievable with filter and impactor technologies. The basic time of flight distributions for nitrate and sulfate are obtained by summing the traces for the appropriate m/z channels, converting to $\log_{10}(D_a)$ space, then normalizing to the MS mode mass loading at the corresponding times.

[45] This simple method of obtaining mass distributions from the TOF data for nitrate and sulfate may be inaccurate for the organic fraction because the ratio of the signals in the different organic m/z channels will vary depending on the speciation of the carbonaceous fraction in the particulate, which will be a strong function of both source and chemical processing. The accompanying paper [*Allan et al.*, 2003]

describes a more robust method for deriving organic mass distributions.

6. Summary

[46] Presented here are the methods used in converting data acquired using an Aerodyne aerosol mass spectrometer into quantitative size and composition resolved mass concentration data for accumulation mode particles. The instrument is capable of operating in two modes, mass spectrum mode, in which information on the composition of the overall aerosol ensemble is obtained, and time of flight mode, from which size-resolved information on particular chemical components is obtained.

[47] Using the techniques described here it is possible to convert measured signals from MS mode into a chemical mass loading by applying calibration values. It is also necessary to apply a correction to account for reductions in electron multiplier performance to continuous data sets to remain quantitative over measurement campaigns. This is calculated by inspecting the instrument's response to gas phase material in the aerosol sample as a function of time.

[48] Averaged TOF signals can be converted into mass distributions in $\log_{10}$ aerodynamic diameter space for particular chemicals using the techniques discussed, through the mathematical transformation of the traces based on calibration data and normalization to the total mass concentrations. It is also possible to quantify the uncertainties in the data produced by both modes of operation. In MS mode, there is an uncertainty in the measurements due to the counting statistics of the individual ions and the uncertainty in the response of the electron multiplier to individual ions. This combined relative uncertainty in a signal is proportional to the square root of the detected ion rate. The error in a TOF signal can be calculated by inspecting the signal in the regions of the trace where no particulate matter is detected and evaluating the standard deviation of the data points. In part 2 of this series [*Allan et al.*, 2003], results derived using these methods from three sampling periods in the U.K. cities of Edinburgh and Manchester are presented and compared with data from other sources.

References

Allan, J. D., et al., Quantitative sampling using an Aerodyne aerosol mass spectrometer, 2, Measurements of fine-particulate chemical composition in two U.K. cities, *J. Geophys. Res.*, *108*, doi:10.1029/2002JD002359, in press, 2003.

Allen, J., and R. K. Gould, Mass-spectrometric analyzer for individual aerosol-particles, *Rev. Sci. Instrum.*, *52*(6), 804–809, 1981.

Allen, J. O., D. P. Fergenson, E. E. Gard, L. S. Hughes, B. D. Morrical, M. J. Kleeman, D. S. Gross, M. E. Galli, K. A. Prather, and G. R. Cass, Particle detection efficiencies of aerosol time of flight mass spectrometers under ambient sampling conditions, *Environ. Sci. Technol.*, *34*(1), 211–217, 2000.

Bley, W. G., Quantitative measurements with quadrupole mass spectrometers—Important specifications for reliable measurements, *Vacuum*, *38*(2), 103–109, 1988.

Charlson, R. J., S. E. Schwartz, J. M. Hales, R. D. Cess, J. A. Coakley, J. E. Hansen, and D. J. Hofmann, Climate forcing by anthropogenic aerosols, *Science*, *255*(5043), 423–430, 1992.

Colvile, R. N., E. J. Hutchinson, J. S. Mindell, and R. F. Warren, The transport sector as a source of air pollution, *Atmos. Environ.*, *35*(9), 1537–1565, 2001.

Department for Environment, Food and Rural Affairs, The air quality strategy for England, Scotland, Wales and Northern Ireland, *Rep. 01EP0538*, London, 2001.

Dockery, D. W., C. A. Pope, X. P. Xu, J. D. Spengler, J. H. Ware, M. E. Fay, B. G. Ferris, and F. E. Speizer, An association between air—pollution and mortality in 6 United States cities, *New Engl. J. Med.*, *329*(24), 1753–1759, 1993.

Environmental Protection Agency, National ambient air quality standards for particulate matter; Final rule, 40 CFR part 50, *Fed. Regist.*, *62*, 138, 1997.

Harrison, R. M., and J. X. Yin, Particulate matter in the atmosphere: Which particle properties are important for its effects on health?, *Sci. Total Environ.*, *249*(1–3), 85–101, 2000.

Hitzenberger, R., A. Berner, H. Giebl, R. Kromp, S. M. Larson, A. Rouc, A. Koch, S. Marischka, and H. Puxbaum, Contribution of carbonaceous material to cloud condensation nuclei concentrations in European background (Mt. Sonnblick) and urban (Vienna) aerosols, *Atmos. Environ.*, *33*(17), 2647–2659, 1999.

Jacob, D. J., Heterogeneous chemistry and tropospheric ozone, *Atmos. Environ.*, *34*(12–14), 2131–2159, 2000.

Jayne, J. T., D. C. Leard, X. F. Zhang, P. Davidovits, K. A. Smith, C. E. Kolb, and D. R. Worsnop, Development of an aerosol mass spectrometer for size and composition analysis of submicron particles, *Aerosol Sci. Technol.*, *33*(1–2), 49–70, 2000.

Jimenez, J. L., J. Bauman, P. Russell, M. Geller, and P. Hamill, Ambient aerosol sampling using the Aerodyne aerosol mass spectrometer, *J. Geophys. Res*, 10.1029/2001JD001213, in press, 2003.

Kane, D. B., and M. V. Johnston, Size and composition biases on the detection of individual ultrafine particles by aerosol mass spectrometry, *Environ. Sci. Technol.*, *34*(23), 4887–4893, 2000.

Künzli, N., et al., Public-health impact of outdoor and traffic-related air pollution: A European assessment, *Lancet*, *356*(9232), 795–801, 2000.

Larssen, S., R. Sluyter, and C. Helmis, Criteria for EUROAIRNET the EEA Air Quality Monitoring and Information Network, *Tech. Rep. 12*, Eur. Environ. Agency, Copenhagen, 1999.

Liu, D. Y., D. Rutherford, M. Kinsey, and K. A. Prather, Real-time monitoring of pyrotechnically derived aerosol particles in the troposphere, *Anal. Chem.*, *69*(10), 1808–1814, 1997.

Liu, P., P. J. Ziemann, D. B. Kittelson, and P. H. McMurry, Generating particle beams of controlled dimensions and divergence, I, Theory of particle motion in aerodynamic lenses and nozzle expansions, *Aerosol Sci. Technol.*, *22*(3), 293–313, 1995a.

Liu, P., P. J. Ziemann, D. B. Kittelson, and P. H. McMurry, Generating particle beams of controlled dimensions and divergence, II, Experimental evaluation of particle motion in aerodynamic lenses and nozzle expansions, *Aerosol Sci. Technol.*, *22*(3), 314–324, 1995b.

Mayer, H., Air pollution in cities, *Atmos. Environ.*, *33*(24–25), 4029–4037, 1999.

McLafferty, F. W., and F. Turecek, *Interpretation of Mass Spectra*, pp. 6–7, Univ. Sci., Mill Valley, Calif., 1993.

McMurry, P. H., A review of atmospheric aerosol measurements, *Atmos. Environ.*, *34*(12–14), 1959–1999, 2000.

Morrical, B. D., D. P. Fergenson, and K. A. Prather, Coupling two-step laser desorption/ionization with aerosol time-of-flight mass spectrometry for the analysis of individual organic particles, *J. Am. Soc. Mass Spectrom.*, *9*(10), 1068–1073, 1998.

Murphy, D. M., and D. S. Thomson, Laser ionization mass-spectroscopy of single aerosol-particles, *Aerosol Sci. Technol.*, *22*(3), 237–249, 1995.

Murphy, D. M., D. S. Thomson, and T. M. J. Mahoney, In situ measurements of organics, meteoritic material, mercury, and other elements in aerosols at 5 to 19 kilometers, *Science*, *282*(5394), 1664–1669, 1998.

Nevalainen, J., and J. Pekkanen, The effect of particulate air pollution on life expectancy, *Sci. Total Environ.*, *217*(1–2), 137–141, 1998.

Prather, K. A., T. Nordmeyer, and K. Salt, Real-time characterization of individual aerosol-particles using time-of-flight mass-spectrometry, *Anal. Chem.*, *66*(9), 1403–1407, 1994.

Ramanathan, V., P. J. Crutzen, J. T. Kiehl, and D. Rosenfeld, Atmosphere—Aerosols, climate, and the hydrological cycle, *Science*, *294*(5549), 2119–2124, 2001.

Ravishankara, A. R., Heterogeneous and multiphase chemistry in the troposphere, *Science*, *276*(5315), 1058–1065, 1997.

Schwartz, J., Air-pollution and daily mortality—A review and meta analysis, *Environ. Res.*, *64*(1), 36–52, 1994.

Seaton, A., W. Macnee, K. Donaldson, and D. Godden, Particulate air-pollution and acute health-effects, *Lancet*, *345*(8943), 176–178, 1995.

Seinfeld, J. H., and S. N. Pandis, *Atmospheric Chemistry and Physics: From Air Pollution To Climate Change*, pp. 414–416, John Wiley, New York, 1998.

Silva, P. J., and K. A. Prather, On-line characterization of individual particles from automobile emissions, *Environ. Sci. Technol.*, *31*(11), 3074–3080, 1997.

Silva, P. J., and K. A. Prather, Interpretation of mass spectra from organic compounds in aerosol time-of-flight mass spectrometry, *Anal. Chem.*, *72*(15), 3553–3562, 2000.

Sinha, M. P., Laser-induced volatilization and ionization of microparticles, *Rev. Sci. Instrum.*, *55*(6), 886–891, 1984.

Stroud, K. A., *Engineering Mathematics: Programmes and Problems*, 893 pp., Macmillan, Old Tappan, N. J., 1987.

Suess, D. T., and K. A. Prather, Mass spectrometry of aerosols, *Chem. Rev.*, *99*(10), 3007–3035, 1999.

Tobias, H. J., and P. J. Ziemann, Compound identification in organic aerosols using temperature—programmed thermal desorption particle beam mass spectrometry, *Anal. Chem.*, *71*(16), 3428–3435, 1999.

White, W. H., and P. T. Roberts, On the nature and origins of visibility-reducing aerosols in the Los Angeles air basin, *Atmos. Environ.*, *11*(9), 803–812, 1977.

Winklmayr, W., G. P. Reischl, A. O. Lindner, and A. Berner, A new electromobility spectrometer for the measurement of aerosol size distributions in the size range from 1 to 1000 Nm, *J. Aerosol Sci.*, *22*(3), 289–296, 1991.

————————

M. R. Alfarra, Department of Chemical Engineering, University of Manchester Institute of Science and Technology, PO Box 88, Manchester M60 1QD, UK. (m.alfarra@student.umist.ac.uk)

J. D. Allan, K. N. Bower, H. Coe, and P. I. Williams, Department of Physics, University of Manchester Institute of Science and Technology, PO Box 88, Manchester M60 1QD, UK. (james.allan@physics.org; keith.bower@umist.ac.uk; hugh.coe@umist.ac.uk; paul.i.williams@umist.ac.uk)

J. T. Jayne and D. R. Worsnop, Aerodyne Research, Inc., 45 Manning Road, Billerica, MA 01821-3976, USA. (jayne@aerodyne.com; worsnop@aerodyne.com)

J. L. Jimenez, Department of Chemistry and Cooperative Institute for Research in the Environmental Sciences (CIRES), University of Colorado, Boulder, CO 80309-0216, USA. (jose.jimenez@colorado.edu)